

# CMB temperature trispectrum of cosmic strings

Mark Hindmarsh\*

*Department of Physics & Astronomy, University of Sussex, Brighton, BN19QH, United Kingdom*

Christophe Ringeval<sup>†</sup> and Teruaki Suyama<sup>‡</sup>

*Theoretical and Mathematical Physics Group, Centre for Particle Physics and Phenomenology,  
Lowain University, 2 Chemin du Cyclotron, 1348 Lowain-la-Neuve, Belgium*

(Dated: August 31, 2018)

We provide an analytical expression for the trispectrum of the Cosmic Microwave Background (CMB) temperature anisotropies induced by cosmic strings. Our result is derived for the small angular scales under the assumption that the temperature anisotropy is induced by the Gott–Kaiser–Stebbins effect. The trispectrum is predicted to decay with a non-integer power-law exponent  $\ell^{-\rho}$  with  $6 < \rho < 7$ , depending on the string microstructure, and thus on the string model. For Nambu–Goto strings, this exponent is related to the string mean square velocity and the loop distribution function. We then explore two classes of wavenumber configuration in Fourier space, the kite and trapezium quadrilaterals. The trispectrum can be of any sign and appears to be strongly enhanced for all squeezed quadrilaterals.

PACS numbers: 98.80.Cq, 98.70.Vc

## I. INTRODUCTION

Although cosmic strings may be of various early universe origins [1–10], being line-like gravitational objects, they induce temperature discontinuities in the CMB through the Gott–Kaiser–Stebbins (GKS) effect [11, 12]. Direct searches for such discontinuities have been performed without success but do provide upper limits to the string tension  $U$  [13–15]. On the other hand, if cosmic strings are added to the standard power-law  $\Lambda$ CDM model [16], it has been shown in Refs. [17, 18] that the CMB data are fitted even better if the fraction of the temperature power spectrum due to strings is about 10% (at  $\ell = 10$ ). Such a fraction of string would even dominate the primary anisotropies of inflationary origin for  $\ell \gtrsim 3000$  [19]. With the advent of the arc-minute resolution CMB experiments and the soon incoming Planck satellite data, it is therefore crucial to develop reliable tests for strings [20], as to understand the non-Gaussian signals. The probability distribution of the fluctuations due to the GKS effect is known to be skewed and has a less steep decay than Gaussian [19], a feature which can be explained in a simple model of kinked string [21]. In Ref. [22], we have studied the temperature bispectrum induced by cosmic strings both analytically and numerically by using Nambu–Goto string simulations. We found good agreement between the analytical and numerical bispectrum for both the overall amplitude and the geometrical factor associated with various triangle configurations of the wavevectors. This agreement suggests that our analytical assumptions are capturing the

relevant non-Gaussian features of a string network and could be used to derive other statistical properties. In this paper, we present new results concerning the trispectrum, i.e. the four-point function of the temperature anisotropy [23]. As pointed out in Ref. [22], the bispectrum is generated only when the background spacetime breaks the time reversal symmetry. Because our universe is expanding, the time reversal symmetry is indeed broken and we get a non-vanishing string bispectrum. On the other hand, the trispectrum can be generated even in Minkowski spacetime and one may naively expect a stronger non-Gaussian signal than for the bispectrum. Motivated by this observation, we provide in this paper an analytical derivation of the string trispectrum and study its dependency for various quadrilateral configurations in Fourier space. Given the fact that analytical predictions and numerical results exhibit good agreement both for the power spectrum [19, 24] and the bispectrum [22], we expect our result here to agree as well with the numerics. Performing such a comparison would however require a significant amount of computing resources which motivated us to leave it for a future work. Our main result can be summarized by Eq. (54). Interestingly, the power-law behaviour of the trispectrum exhibits a non-integer exponent which can be related to the small scale behaviour of the string tangent vector correlator. In the framework of Nambu–Goto strings, this exponent is related to the mean square string velocity [25, 26] and to the scaling loop distribution function [27, 28]. The paper is organised as follows. In the next section we briefly recall the assumptions at the basis of our analytical approach and derive the trispectrum in Sec. III. As an illustration, we apply our result to some specific quadrilaterals in Sec. IV and exhibit some configurations that leads to a divergent trispectrum. They should provide the cleanest way to look for a non-Gaussian string signal.

---

\*Electronic address: m.b.hindmarsh@sussex.ac.uk

<sup>†</sup>Electronic address: christophe.ringeval@uclouvain.be

<sup>‡</sup>Electronic address: teruaki.suyama@uclouvain.be

## II. TEMPERATURE ANISOTROPY FROM COSMIC STRINGS

In this section, we briefly review the general basics needed to calculate  $N$ -point function of  $\Theta \equiv \Delta T/T_{\text{CMB}}$  at small angular scales. To study the correlation functions in the small angle limit, it is enough to consider  $\Theta$  on the small patch of the sky. Then we can approximate this patch as two-dimensional Euclidean space, which simplifies the calculations. In this limit, the integrated Sachs–Wolfe effect generated by cosmic strings yields the temperature anisotropy in the light-cone gauge [24]

$$-k^2 \Theta_{\mathbf{k}} = i\varepsilon k_A \int d\sigma \dot{X}^A(\sigma) e^{i\mathbf{k} \cdot \mathbf{X}(\sigma)}, \quad (1)$$

where we have defined

$$\varepsilon = 8\pi G U, \quad (2)$$

and  $X^A$  ( $A = 1, 2$ ) is the two-dimensional string position vector perpendicular to the line of sight. We implicitly assume a summation on the repeated indices. It is now clear that the power spectrum, bispectrum, and higher order correlators can be evaluated in terms of correlation functions of the string network, as projected onto our backward light-cone. In order to evaluate the statistical quantities constructed over  $\Theta_{\mathbf{k}}$ , the correlation functions of  $\dot{X}^A$  and  $\dot{X}^B$  have to be known. However, because  $\Theta_{\mathbf{k}}$  depends on  $\dot{X}^A$  and  $\dot{X}^B$  in a non-trivial manner, it is extremely difficult to derive meaningful consequences for the correlation functions without imposing additional conditions on the string correlators. In this paper, as done in Refs. [22, 24] we therefore assume that both  $\dot{X}^A$  and  $\dot{X}^B$  obey Gaussian statistics, and this drastically simplifies our calculations. All the correlation functions of  $\Theta_{\mathbf{k}}$  can now be written in terms of the two-point functions only. Using the same notation as in Ref. [24], the two-point functions of the string correlators are

$$\begin{aligned} \langle \dot{X}^A(\sigma) \dot{X}^B(\sigma') \rangle &= \frac{1}{2} \delta^{AB} V(\sigma - \sigma'), \\ \langle \dot{X}^A(\sigma) \dot{X}^B(\sigma') \rangle &= \frac{1}{2} \delta^{AB} M(\sigma - \sigma'), \\ \langle \dot{X}^A(\sigma) \dot{X}^B(\sigma') \rangle &= \frac{1}{2} \delta^{AB} T(\sigma - \sigma'). \end{aligned} \quad (3)$$

Note that an appearance of a term like  $\epsilon^{AB} N(\sigma - \sigma')$  in the mixed correlator  $\langle \dot{X}^A \dot{X}^B \rangle$ , where  $\epsilon^{AB}$  is the anti-symmetric tensor with  $\epsilon^{12} = 1$ , is forbidden due to the symmetry. As for the bispectrum, we also introduce the correlator [22]

$$\Gamma(\sigma - \sigma') \equiv \langle [\mathbf{X}(\sigma) - \mathbf{X}(\sigma')]^2 \rangle \quad (4)$$

$$= \int_{\sigma'}^{\sigma} d\sigma_1 \int_{\sigma'}^{\sigma} d\sigma_2 T(\sigma_1 - \sigma_2). \quad (5)$$

The leading terms are given by [22]

$$\begin{aligned} V(\sigma) &\rightarrow \begin{cases} \bar{v}^2 & \sigma \rightarrow 0 \\ 0 & \sigma \rightarrow \infty \end{cases}, \\ \Gamma(\sigma) &\rightarrow \begin{cases} \bar{t}^2 \sigma^2 & \sigma \rightarrow 0 \\ \hat{\xi} \sigma & \sigma \rightarrow \infty \end{cases}, \end{aligned} \quad (6)$$

where we have defined

$$\hat{\xi} = \Gamma'(\infty), \quad \bar{v}^2 = \langle \dot{\mathbf{X}}^2 \rangle, \quad \bar{t}^2 = \langle \dot{\mathbf{X}}^2 \rangle. \quad (7)$$

The correlation length  $\hat{\xi}$  is the projected correlation length on the backward light-cone,  $\bar{t}^2$  is the mean square projected tangent vector (of order unity),  $\bar{v}^2$  is the mean square projected velocity (again of order unity).

## III. TEMPERATURE TRISPECTRUM

In the flat sky approximation the four-point temperature correlation function is defined as

$$\begin{aligned} \langle \Theta_{\mathbf{k}_1} \Theta_{\mathbf{k}_2} \Theta_{\mathbf{k}_3} \Theta_{\mathbf{k}_4} \rangle &= T(\mathbf{k}_1, \mathbf{k}_2, \mathbf{k}_3, \mathbf{k}_4) (2\pi)^2 \\ &\times \delta(\mathbf{k}_1 + \mathbf{k}_2 + \mathbf{k}_3 + \mathbf{k}_4). \end{aligned} \quad (8)$$

Using Eq. (1) and a formal area factor  $\mathcal{A} = (2\pi)^2 \delta(0)$ , the trispectrum<sup>1</sup> can be written as

$$\begin{aligned} T(\mathbf{k}_1, \mathbf{k}_2, \mathbf{k}_3, \mathbf{k}_4) &= \varepsilon^4 \frac{1}{\mathcal{A}} \delta_{AA} \delta_{BB} \delta_{CC} \delta_{DD} \frac{k_1^A k_2^B k_3^C k_4^D}{k_1^2 k_2^2 k_3^2 k_4^2} \\ &\times \int d\sigma_1 d\sigma_2 d\sigma_3 d\sigma_4 \langle \dot{X}_1^A \dot{X}_2^B \dot{X}_3^C \dot{X}_4^D e^{i\delta^{ab} \mathbf{k}_a \cdot \mathbf{X}_b} \rangle, \end{aligned} \quad (9)$$

with  $\dot{X}_a^A = \dot{X}^A(\sigma_a)$ ,  $(a, b) \in \{1, 2, 3, 4\}$  and  $\mathbf{k}_1 + \mathbf{k}_2 + \mathbf{k}_3 + \mathbf{k}_4 = 0$ . We now assume Gaussian statistics and define

$$\mathcal{C}^{ABCD} = \dot{X}_1^A \dot{X}_2^B \dot{X}_3^C \dot{X}_4^D, \quad (10)$$

$$\mathcal{D} = \delta^{ab} \mathbf{k}_a \cdot \mathbf{X}_b. \quad (11)$$

The ensemble average in Eq. (9) can be expressed in terms of the two-point functions only

$$\begin{aligned} \langle \mathcal{C}^{ABCD} e^{i\mathcal{D}} \rangle &= \left[ \langle \mathcal{C}^{ABCD} \rangle + \langle \dot{X}_1^A \dot{X}_2^B \rangle \langle \dot{X}_3^C \mathcal{D} \rangle + \text{O} \right. \\ &\quad \left. + \langle \dot{X}_1^A \mathcal{D} \rangle \langle \dot{X}_2^B \mathcal{D} \rangle \langle \dot{X}_3^C \mathcal{D} \rangle \langle \dot{X}_4^D \mathcal{D} \rangle \right] e^{-\frac{1}{2} \langle \mathcal{D}^2 \rangle}, \end{aligned} \quad (12)$$

where  $\text{O}$  denotes permutations of the labels  $\{1, 2, 3\}$ . Expressing  $\mathbf{X}(\sigma)$  in terms of  $\dot{\mathbf{X}}(\sigma)$  makes clear that all terms but the first involve the mixed correlators

<sup>1</sup> Notice that our denomination ‘‘trispectrum’’ here stands for the four-point function and contains the unconnected part. This one is however non-vanishing only for parallelogram configurations of the wave vectors.

$\langle \dot{\mathbf{X}}(\sigma) \dot{\mathbf{X}}(\sigma') \rangle$ ). Since they give a small contribution compared to the others, we will not consider these extra terms in the following. A more detailed calculation would show that they induce corrections to the trispectrum scaling relative to the first term as  $1/k$  and  $1/k^2$ , respectively, and therefore are negligible at small angular scales. The trispectrum can be approximated as

$$T(\mathbf{k}_1, \mathbf{k}_2, \mathbf{k}_3, \mathbf{k}_4) \simeq \varepsilon^4 \frac{1}{\mathcal{A}} \delta_{A\bar{A}} \delta_{B\bar{B}} \delta_{C\bar{C}} \delta_{D\bar{D}} \frac{k_1^{\bar{A}} k_2^{\bar{B}} k_3^{\bar{C}} k_4^{\bar{D}}}{k_1^2 k_2^2 k_3^2 k_4^2} \times \int d\sigma_1 d\sigma_2 d\sigma_3 d\sigma_4 \langle \mathcal{C}^{ABCD} \rangle e^{-\frac{1}{2} \langle \mathcal{D}^2 \rangle}. \quad (13)$$

In terms of the two-point functions introduced in Sec. II,

$$\langle \mathcal{C}^{ABCD} \rangle = \frac{1}{4} \delta^{AB} \delta^{CD} V(\sigma_{12}) V(\sigma_{34}) + \frac{1}{4} \delta^{AC} \delta^{DB} V(\sigma_{31}) V(\sigma_{42}) + \frac{1}{4} \delta^{AD} \delta^{BC} V(\sigma_{14}) V(\sigma_{23}), \quad (14)$$

where  $\sigma_{ab} \equiv \sigma_a - \sigma_b$ . As for  $\langle \mathcal{D}^2 \rangle$ , replacing  $\mathbf{k}_4$  with  $-\mathbf{k}_1 - \mathbf{k}_2 - \mathbf{k}_3$ , one gets

$$\langle \mathcal{D}^2 \rangle = \left\langle (\mathbf{k}_1 \cdot \mathbf{X}_{14} + \mathbf{k}_2 \cdot \mathbf{X}_{24} + \mathbf{k}_3 \cdot \mathbf{X}_{34})^2 \right\rangle, \quad (15)$$

where  $\mathbf{X}_{ab} \equiv \mathbf{X}_a - \mathbf{X}_b$ . As in Ref. [22], one can show that

$$\langle \mathbf{X}_{14} \cdot \mathbf{X}_{24} \rangle = \frac{1}{2} [\Gamma(\sigma_{14}) + \Gamma(\sigma_{24}) - \Gamma(\sigma_{12})], \quad (16)$$

which can be used to transform Eq. (15) into a manifestly symmetric expression

$$\langle \mathcal{D}^2 \rangle = \frac{1}{2} \sum_{a < b} \kappa_{ab} \Gamma(\sigma_{ab}), \quad (17)$$

with

$$\kappa_{ab} \equiv -\mathbf{k}_a \cdot \mathbf{k}_b. \quad (18)$$

At this point, plugging this expression into Eq. (13) and performing the integrations along the lines done for the bispectrum is not possible (see Ref. [22]). Indeed, since the  $\mathbf{k}_a$  are forming a quadrilateral, contrary to the bispectrum triangle configurations, all the  $\kappa_{ab}$  cannot be positive thereby preventing some of the Gaussian integrals to be performed.

We can nevertheless perform one integration by switching to the more convenient integration variables  $\sigma_{14}$ ,  $\sigma_{24}$ ,  $\sigma_{34}$  and  $\sigma_4$ . The Jacobian is unity and Eq. (17) can be rewritten in a non-symmetric form depending only on three of the variables:

$$\langle \mathcal{D}^2 \rangle = -\frac{1}{2} \sum_{i=1}^3 \sum_{j=1}^3 \kappa_{ij} \Omega_{ij}, \quad (19)$$

where

$$\Omega_{ij} = \frac{1}{2} [\Gamma(\sigma_{i4}) + \Gamma(\sigma_{j4}) - \Gamma(\sigma_{i4} - \sigma_{j4})]. \quad (20)$$

From Eqs. (13) and (14), we find that the integrand does not depend on  $\sigma_4$  and the integration yields a factor equal to the total length of the strings  $L$  in the area  $\mathcal{A}$ . In order to perform the integration over the other variables, one can again use the small angle approximation where all the  $k_a$  are taken to be sufficiently large. The dominant parts then come from the small  $\sigma$  length scales, the contributions from other regions being exponentially suppressed. This suggests we should Taylor-expand the two-point functions around  $\sigma = 0$ . At leading order, using Eq. (6), one gets  $\Omega_{ij} \simeq \bar{t}^2 \sigma_{i4} \sigma_{j4}$  implying that  $\langle \mathcal{D}^2 \rangle$  is a quadratic form in the variables  $\sigma_{i4}$ . However, it exhibits a vanishing eigenvalue and the Gaussian integral cannot be extended to infinity since there is one direction of integration along which the exponent  $\kappa_{ij} \Omega_{ij}$  remains null. Let us notice that the situation is different than for the variable  $\sigma_4$ ; the correlators are indeed function of such a flat direction whereas they do not depend on  $\sigma_4$ . In order to get a sensible result, we therefore need to include higher order corrections to the two-point functions.

The behavior of  $T(\sigma)$  at small scales is not trivial and many analytical works have been devoted to its determination [25, 26, 29, 30]. In the Polchinski and Rocha model of Ref. [25], the next-to-leading order terms of the correlators  $\langle \dot{\mathbf{X}} \cdot \dot{\mathbf{X}} \rangle$  and  $\langle \dot{\mathbf{X}} \cdot \dot{\mathbf{X}} \rangle$  have a non-integer exponent. These correlators match with Abelian string simulations performed in Ref. [31] and can also be used to analytically derive the cosmic string loops distribution expected in an expanding universe. As shown in Ref. [28], these results also match with the scaling loop distribution observed in the Nambu–Goto numerical simulations of Ref. [27]. As a result, we assume in the following a non-analytical behaviour for  $T(\sigma)$  at small scales

$$T(\sigma) \simeq \bar{t}^2 - c_1 \left( \frac{\sigma}{\bar{\xi}} \right)^{2\chi}. \quad (21)$$

Notice that we are working in the light-cone gauge and therefore leave  $c_1$  and  $\chi$  as undetermined parameters since they cannot be straightforwardly inferred from the numerics performed in the temporal gauge. Nevertheless, because the correlation should be smaller as  $\sigma$  becomes larger,  $c_1$  must be positive. Let us also mention the recent work of Ref. [26] suggesting that at very small length scales the correlator should become again analytic (with  $\chi = 1/2$ ), i.e. that Eq. (21) would hold only for  $\sigma > \sigma_c$ . However, as discussed in this reference,  $\sigma_c$  is shrinking with time in an expanding universe and at the times of observational interest, Eq. (21) is expected to be valid on all the length scales we are interested in.

With this next-to-leading order form of  $T(\sigma)$ , one obtains

$$\Gamma(\sigma) \simeq \bar{t}^2 \sigma^2 - \frac{c_1}{(1 + \chi)(1 + 2\chi) \bar{\xi}^{2\chi}} \sigma^{2\chi+2}, \quad (22)$$

and Eq. (19) reads

$$\langle \mathcal{D}^2 \rangle = -\frac{1}{2} \bar{t}^2 \kappa^{ij} \sigma_{i4} \sigma_{j4} + c_1 \frac{\kappa^{ij} \phi(\sigma_{i4}, \sigma_{j4})}{2(2\chi+1)(2\chi+2)\hat{\xi}^{2\chi}}, \quad (23)$$

where

$$\phi(\sigma_{i4}, \sigma_{j4}) \equiv (|\sigma_{i4}|^{2\chi+2} + |\sigma_{j4}|^{2\chi+2} - |\sigma_{i4} - \sigma_{j4}|^{2\chi+2}). \quad (24)$$

We can perform a linear coordinate transformation by introducing the set of orthonormal unit vectors ( $\mathbf{e}_1, \mathbf{e}_2, \mathbf{e}_1 \wedge \mathbf{e}_2$ ) and define three new coordinates  $\chi_1, \chi_2$  and  $\chi_3$  along these directions:

$$\begin{aligned} \chi_1 &\equiv \delta^{ij} (\mathbf{e}_1 \cdot \mathbf{k}_i) \sigma_{j4}, & \chi_2 &\equiv \delta^{ij} (\mathbf{e}_2 \cdot \mathbf{k}_i) \sigma_{j4}, \\ \chi_3 &\equiv \varepsilon^{ijl} (\mathbf{e}_1 \cdot \mathbf{k}_i) (\mathbf{e}_2 \cdot \mathbf{k}_j) \sigma_{l4}. \end{aligned} \quad (25)$$

We then have

$$\begin{aligned} \langle \mathcal{D}^2 \rangle &= \frac{1}{2} \bar{t}^2 (\chi_1^2 + \chi_2^2) + \frac{c_1}{2(2\chi+1)(2\chi+2)\hat{\xi}^{2\chi}} \\ &\quad \times \kappa^{ij} \phi[\sigma_{i4}(\vec{\chi}), \sigma_{j4}(\vec{\chi})]. \end{aligned} \quad (26)$$

The third coordinate  $\chi_3$  appears in  $\langle \mathcal{D}^2 \rangle$  only when the next-to-leading order terms in  $T(\sigma)$  are taken into account, which is consistent with the observation that there is a flat direction at leading order. The last term in the previous equation contributes little to the integrations over  $\chi_1$  and  $\chi_2$ . Hence we can safely say that the only non-vanishing component of  $\vec{\chi}$  in the last term is  $\chi_3$ . This is equivalent to include the next-to-leading order corrections only along the flat direction, i.e. for

$$\sigma_{l4} = \frac{1}{\mathcal{J}} \varepsilon_l^{ij} (\mathbf{e}_1 \cdot \mathbf{k}_i) (\mathbf{e}_2 \cdot \mathbf{k}_j) \chi_3, \quad (27)$$

where  $\mathcal{J}$  is the Jacobian of the transformation given by Eq. (25). Then, introducing the outer product coordinates by

$$\begin{aligned} w_{ij} &\equiv (\mathbf{e}_1 \cdot \mathbf{k}_i) (\mathbf{e}_2 \cdot \mathbf{k}_j) - (\mathbf{e}_1 \cdot \mathbf{k}_j) (\mathbf{e}_2 \cdot \mathbf{k}_i) \\ &= \pm \sqrt{k_i^2 k_j^2 - \kappa_{ij}^2}, \end{aligned} \quad (28)$$

one can show that

$$\begin{aligned} \kappa_{11} \phi(\sigma_{14}, \sigma_{14}) &= -\frac{2}{\mathcal{J}^{2\chi+2}} k_1^2 |w_{23}|^{2\chi+2} \chi_3^{2\chi+2}, \\ \kappa_{12} \phi(\sigma_{14}, \sigma_{24}) &= -\frac{1}{\mathcal{J}^{2\chi+2}} \kappa_{12} (|w_{23}|^{2\chi+2} - |w_{34}|^{2\chi+2} \\ &\quad + |w_{31}|^{2\chi+2}) \chi_3^{2\chi+2}, \end{aligned} \quad (29)$$

and other permutations. Finally, making use of identities such as

$$\kappa_{12} + \kappa_{13} + \kappa_{14} = \mathbf{k}_1^2, \quad (30)$$

one gets

$$\begin{aligned} \langle \mathcal{D}^2 \rangle &= \frac{1}{2} \bar{t}^2 (\chi_1^2 + \chi_2^2) + \frac{c_1}{(2\chi+1)(2\chi+2)\hat{\xi}^{2\chi}} Y^2 \\ &\quad \times \left( \frac{\chi_3}{\mathcal{J}} \right)^{2\chi+2}, \end{aligned} \quad (31)$$

with

$$Y^2 \equiv -\kappa_{12} |w_{34}|^{2\chi+2} + \circlearrowleft. \quad (32)$$

Notice that  $Y^2 \geq 0$  for any quadrilateral because of the inequality  $\langle \mathcal{D}^2 \rangle \geq 0$ . With these new variables, the trispectrum reads

$$\begin{aligned} T(\mathbf{k}_1, \mathbf{k}_2, \mathbf{k}_3, \mathbf{k}_4) &\simeq \varepsilon^4 \frac{L}{4A k_1^2 k_2^2 k_3^2 k_4^2} \int d\chi_1 d\chi_2 \frac{d\chi_3}{\mathcal{J}} \\ &\quad \{ \kappa_{12} \kappa_{34} V[\sigma_{12}(\vec{\chi})] V[\sigma_{34}(\vec{\chi})] + \circlearrowleft \} e^{-\frac{1}{2} \langle \mathcal{D}^2 \rangle}. \end{aligned} \quad (33)$$

At this stage, the Gaussian integrations over  $\chi_1$  and  $\chi_2$  are always finite, and for large enough wave numbers, i.e.  $k\hat{\xi} \gg 1$ , we can safely extend the integration range to infinity and also put  $\chi_1 = \chi_2 = 0$  in  $V(\sigma_{ij})$ . From Eq. (31), the integration over  $\chi_1$  and  $\chi_2$  yields

$$\begin{aligned} T(\mathbf{k}_1, \mathbf{k}_2, \mathbf{k}_3, \mathbf{k}_4) &\simeq \frac{\pi \varepsilon^4}{\bar{t}^2} \frac{L}{A k_1^2 k_2^2 k_3^2 k_4^2} \int d \left( \frac{\chi_3}{\mathcal{J}} \right) \\ &\quad \times \left\{ \kappa_{12} \kappa_{34} V \left( w_{34} \frac{\chi_3}{\mathcal{J}} \right) V \left( w_{12} \frac{\chi_3}{\mathcal{J}} \right) + \circlearrowleft \right\} \\ &\quad \times \exp \left[ -c_2 Y^2 \left( \frac{\chi_3}{\mathcal{J}} \right)^{2\chi+2} \right], \end{aligned} \quad (34)$$

with

$$c_2 \equiv \frac{c_1}{2\hat{\xi}^{2\chi} (2\chi+1)(2\chi+2)}. \quad (35)$$

The integration over  $\chi_3$  may, *a-priori*, be performed in the same way. However, from Eq. (32), one can show that there is some particular configurations for which  $Y$  vanishes (parallelograms). As a result, one cannot push the integration up to infinity for those and one has to integrate only over the total string length. Notice that the integral depends on  $L$  only for the particular parallelogram configurations. As soon as  $Y^2 \neq 0$ , the small angle limit implies that  $Y^2$  is large and the exponential function takes non-vanishing values only around vanishing  $\chi_3$ . For this reason, we separate our analysis in two cases and first focus on the parallelogram case.

### A. Parallelogram configurations $Y^2 = 0$

For parallelograms, the two opposite wavevectors forming the quadrilateral are anti-parallel and  $Y^2$  strictly vanishes. Without loss of generality, we assume  $\mathbf{k}_1 + \mathbf{k}_3 = 0$  and  $\mathbf{k}_2 + \mathbf{k}_4 = 0$ . In this case, one has  $w_{13} = w_{24} = 0$  and we define

$$w = w_{12} = w_{23} = k_1 k_2 \sin \theta = k_2 k_3 \sin \theta. \quad (36)$$

The integral in Eq. (34) can be evaluated along the flat direction  $\chi_3/\mathcal{J}$ , which is given by Eq. (27),

$$\sigma_{14} = \sigma_{34} = w \frac{\chi_3}{\mathcal{J}}, \quad \sigma_{24} = 0. \quad (37)$$

The integration range on  $\chi_3/\mathcal{J}$  is thus  $[-\Lambda, \Lambda]$  where

$$\Lambda = \frac{L}{2|w|}. \quad (38)$$

From Eq. (34), the trispectrum simplifies to

$$\begin{aligned} T_0(\mathbf{k}_1, \mathbf{k}_2, \mathbf{k}_3, \mathbf{k}_4) &= \frac{\pi \varepsilon^4 \bar{v}^4}{\bar{t}^2} \frac{L^2}{\mathcal{A} k_1 k_2 k_3 k_4 |w|} \\ &\times \left[ 1 + 2 \cos^2(\theta) \frac{1}{L/2} \int_0^{L/2} \frac{V^2(\sigma)}{\bar{v}^4} d\sigma \right] \\ &\simeq \frac{\pi \varepsilon^4 \bar{v}^4}{\bar{t}^2} \frac{L^2}{\mathcal{A} k_1^3 k_2^3 |\sin \theta|}, \end{aligned} \quad (39)$$

where we have neglected the integral in the last line. Since the correlator  $V^2(\sigma)$  is expected to be small at distances larger than the typical correlation length  $\hat{\xi}$ , this integral can be approximated by

$$\frac{1}{L/2} \int_0^{\hat{\xi}} \frac{V^2(\sigma)}{\bar{v}^4} d\sigma = \frac{2}{L \bar{v}^4} \hat{\xi} V^2(\sigma_0) \leq 2 \frac{\hat{\xi}}{L} \ll 1, \quad (40)$$

where we have used the mean value theorem with  $\sigma_0 \in [0, \hat{\xi}]$ . Under the scaling transformation  $\mathbf{k}_a \rightarrow b\mathbf{k}_a$ , the parallelogram trispectrum in Eq. (39) scales as

$$T_0(b\mathbf{k}_1, b\mathbf{k}_2, b\mathbf{k}_3, b\mathbf{k}_4) = b^{-6} T_0(\mathbf{k}_1, \mathbf{k}_2, \mathbf{k}_3, \mathbf{k}_4). \quad (41)$$

For parallelograms, it is important to recall that the trispectrum always gets a contribution from the unconnected part of the four-point function, which is purely given by a Gaussian distribution,

$$T_0^{\text{uc}}(\mathbf{k}_1, \mathbf{k}_2, \mathbf{k}_3, \mathbf{k}_4) = \mathcal{A} P(k_1) P(k_2) + \circ. \quad (42)$$

As shown in Ref. [24], the power spectrum is given by

$$P(k) = \sqrt{\pi} \varepsilon^2 \frac{L \bar{v}^2}{\mathcal{A} \bar{t} k^3}, \quad (43)$$

and the unconnected part of the trispectrum also scales as  $b^{-6}$ . Therefore the non-Gaussian contributions for parallelogram configurations remain of the same order of magnitude as the Gaussian ones, with the exception of the squeezed limit  $\theta \rightarrow 0$ . As we will see in the following, all other quadrilateral configurations have a scaling law which is different than Eq. (41).

## B. Quadrilateral configurations with $Y^2 \gg 1$

In this case, the integrand in Eq. (34) takes non vanishing values only around  $\chi_3 = 0$  and we can safely extend the integration range over  $\chi_3/\mathcal{J}$  to infinity, as we have done for  $\chi_1$  and  $\chi_2$ . One gets

$$\begin{aligned} T_\infty(\mathbf{k}_1, \mathbf{k}_2, \mathbf{k}_3, \mathbf{k}_4) &\simeq \varepsilon^4 \frac{\bar{v}^4}{\bar{t}^2} \frac{L \hat{\xi}}{\mathcal{A}} \left( c_1 \hat{\xi}^2 \right)^{-1/(2\chi+2)} f(\chi) \\ &\times g(\mathbf{k}_1, \mathbf{k}_2, \mathbf{k}_3, \mathbf{k}_4). \end{aligned} \quad (44)$$

The function  $f(\chi)$  is a number depending only on the power-law exponent  $\chi$

$$f(\chi) = \frac{\pi}{\chi+1} \Gamma\left(\frac{1}{2\chi+2}\right) [4(2\chi+1)(\chi+1)]^{1/(2\chi+2)}, \quad (45)$$

and  $g(\{\mathbf{k}_a\})$  is the trispectrum geometrical factor

$$\begin{aligned} g(\mathbf{k}_1, \mathbf{k}_2, \mathbf{k}_3, \mathbf{k}_4) &= \frac{\kappa_{12}\kappa_{34} + \kappa_{13}\kappa_{24} + \kappa_{14}\kappa_{23}}{k_1^2 k_2^2 k_3^2 k_4^2} \\ &\times \left[ -\kappa_{12} (k_3^2 k_4^2 - \kappa_{34}^2)^{\chi+1} + \circ \right]^{-1/(2\chi+2)}. \end{aligned} \quad (46)$$

From Eq. (44), we can derive various consequences worth mentioning. First, the sign of the trispectrum is completely determined by the geometrical factor in Eq. (46), which is manifestly symmetric under the permutation of two different wavevectors. The factor

$$-\kappa_{12} (k_3^2 k_4^2 - \kappa_{34}^2)^{\chi+1} + \circ \quad (47)$$

is always positive or zero. Also  $f(\chi)$  (for a physically reasonable range of  $\chi$ ) and  $c_1$  are positive. Therefore the sign of the trispectrum is given by the factor

$$\kappa_{12}\kappa_{34} + \kappa_{13}\kappa_{24} + \kappa_{14}\kappa_{23}, \quad (48)$$

which can be positive or negative according to the quadrilateral under scrutiny.

Secondly, under the scaling transformation  $\mathbf{k}_a \rightarrow b\mathbf{k}_a$ , the geometric factor scales as

$$g(b\mathbf{k}_1, b\mathbf{k}_2, b\mathbf{k}_3, b\mathbf{k}_4) = b^{-\rho} g(\mathbf{k}_1, \mathbf{k}_2, \mathbf{k}_3, \mathbf{k}_4), \quad (49)$$

with

$$\rho = 6 + \frac{1}{\chi+1}. \quad (50)$$

Contrary to the case of the power spectrum, of the bispectrum, and of the parallelogram configurations, the leading term of the trispectrum scales with a non-integer power-law exponent. For  $\chi > 0$ , the trispectrum decays slightly faster at small scales than the bispectrum. Let us recap that in the temporal gauge, the string tangent vector correlation function exponent  $\chi$  is a small quantity related to the expansion rate of the scale factor and to the mean square velocity of strings [25]. This is certainly also the case in the light-cone gauge and one may be able to use the trispectrum to distinguish between different models of strings. For instance, in Abelian Higgs numerical simulations, the strong back-reaction induced by scalar and gauge radiation produces a mean square velocity lower than in classical Nambu-Goto simulations [31, 32]. Meanwhile, the loop distribution observed in Nambu-Goto simulations has a power-law exponent which is uniquely given by  $\chi$  [27]. Interestingly, the scaling exponent is different from the one associated with parallelogram configurations. These two different scaling behaviors may actually be used to distinguish the trispectrum by cosmic string with the one generated by other sources.

### C. Interpolating trispectrum for all quadrilaterals

When  $Y^2 \simeq 0$  but non-vanishing, i.e. for quadrilaterals close to parallelograms, one cannot push the integration range in Eq. (34) to infinity. Contrary to the case  $Y^2 = 0$ , the integration over  $\chi_3/\mathcal{J}$  cannot be performed explicitly in this case. Nevertheless, we can make some approximations. First, for configurations close to parallelograms, two of the  $w_{ij}$  quantities are expected to be small, say  $w_{13}$  and  $w_{24}$ . For those, one can replace the  $V(\sigma)$  functions in Eq. (34) by  $\bar{v}^2$ . On the other hand, one expects the other  $w_{mn}$  factors to be large and Eq. (34) has terms involving the product  $V(\sigma)V(\sigma')$ . As for the parallelograms, we expect those to be at most of the order  $\bar{v}^4 \hat{\xi}/L$ , which can be neglected compared to the terms in  $\bar{v}^4$ . With an integration range over  $\chi_3/\mathcal{J}$  given by  $[-\Lambda, \Lambda]$ , where  $\Lambda(\mathbf{k}_a, L)$  has still to be specified, performing the last integration over  $\chi_3$  yields

$$T_{w_{13}w_{24}}(\mathbf{k}_1, \mathbf{k}_2, \mathbf{k}_3, \mathbf{k}_4) \simeq \varepsilon^4 \frac{\bar{v}^4 L \hat{\xi}}{f^2 \mathcal{A}} (c_1 \hat{\xi}^2)^{-1/(2\chi+2)} f(\chi) \times \gamma_n \left( \frac{1}{2\chi+2}, c_2 Y^2 \Lambda^{2\chi+2} \right) \frac{\kappa_{13}\kappa_{24}}{k_1^2 k_2^2 k_3^2 k_4^2} Y^{-2/(2\chi+2)}, \quad (51)$$

where  $\gamma_n(a, x)$  denotes the normalised incomplete lower gamma function

$$\gamma_n(a, x) \equiv \frac{\gamma(a, x)}{\Gamma(a)}. \quad (52)$$

In the limit  $Y^2 \rightarrow 0$ , this expression matches with Eq. (39) for  $\Lambda = L/(2|w_{12}|)$ . In order to interpolate between Eqs. (39) and (44) we can replace the geometrical factor in Eq. (51) by the factor  $g(\{\mathbf{k}_a\})$  and chose the cutoff  $\Lambda$  to be

$$\Lambda \equiv \frac{2L}{|w_{12}| + |w_{13}| + |w_{14}| + |w_{23}| + |w_{24}| + |w_{34}|} \times \frac{k_1 k_2 k_3 k_4}{\kappa_{12}\kappa_{34} + \kappa_{13}\kappa_{24} + \kappa_{14}\kappa_{23}}. \quad (53)$$

Our interpolation formula for the trispectrum finally reads

$$T(\mathbf{k}_1, \mathbf{k}_2, \mathbf{k}_3, \mathbf{k}_4) \simeq \varepsilon^4 \frac{\bar{v}^4 L \hat{\xi}}{f^2 \mathcal{A}} (c_1 \hat{\xi}^2)^{-1/(2\chi+2)} f(\chi) \times \gamma_n \left( \frac{1}{2\chi+2}, c_2 Y^2 \Lambda^{2\chi+2} \right) g(\mathbf{k}_1, \mathbf{k}_2, \mathbf{k}_3, \mathbf{k}_4), \quad (54)$$

with  $\Lambda$  given by Eq. (53) and  $g(\{\mathbf{k}_a\})$  by Eq. (46). For  $Y^2$  large, the gamma function is close to one and we recover Eq. (44). The limit  $Y^2 = 0$  gives again the leading order of Eq. (39).

## IV. GEOMETRICAL FACTORS OF SYMMETRIC QUADRILATERALS

In this section, we explore the dependency of the trispectrum geometrical factor given by Eq. (46) for some

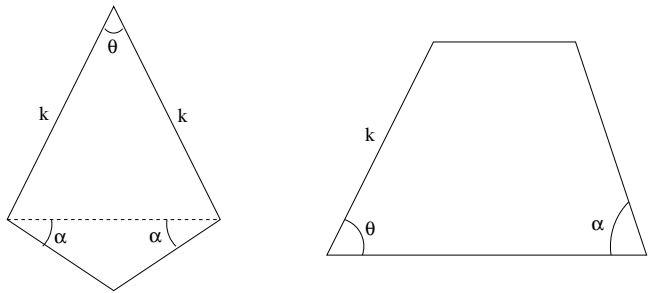


FIG. 1: Quadrilateral configurations for the trispectrum wavenumbers. The left is referred to as the “kite” quadrilaterals with two adjacent sides of equal length and the other two sides also of equal length. The right quadrilateral is a “trapezium” which is defined to have two opposite sides parallel.

symmetric quadrilateral configurations of the wavevectors.

### A. Kite configurations

Let us first consider a quadrilateral like the one given in Fig. 1 (left). From Eq. (32), one gets

$$Y^2 = k^{6+4\chi} y^2(\theta, \alpha), \quad (55)$$

with

$$y^2(\theta, \alpha) = [\sin^2(\theta/2)]^{1+\chi} \times \left\{ 2 \sin(\theta/2) \frac{\sin(\alpha - \theta/2)}{\cos \alpha} \times \left[ \frac{\cos^2(\alpha - \theta/2)}{\cos^2 \alpha} \right]^{1+\chi} - 2 \sin(\theta/2) \frac{\sin(\alpha + \theta/2)}{\cos \alpha} \left[ \frac{\cos^2(\alpha + \theta/2)}{\cos^2 \alpha} \right]^{1+\chi} + 4^{1+\chi} \sin^2(\theta/2) [\cos^2(\theta/2)]^{1+\chi} \frac{\cos(2\alpha)}{\cos^2(\alpha)} - 4^{1+\chi} \cos(\theta) [\sin^2(\theta/2) \tan^2(\alpha)]^{1+\chi} \right\}. \quad (56)$$

From Eq. (46), the geometrical factor reads

$$g(\mathbf{k}_1, \mathbf{k}_2, \mathbf{k}_3, \mathbf{k}_4) = \frac{\cos^2(\alpha) [1 - 2 \cos(2\alpha) \cos(\theta)]}{\sin^2(\theta/2)} \times \frac{1}{k^\rho y^{2/(2+2\chi)}}. \quad (57)$$

As expected from the trispectrum scaling law, the kite trispectrum decays as  $1/k^\rho$  at small angular scales. The overall amplitude is however amplified for squeezed configurations and diverges for  $\theta \rightarrow 0$ . For  $\theta$  small, the

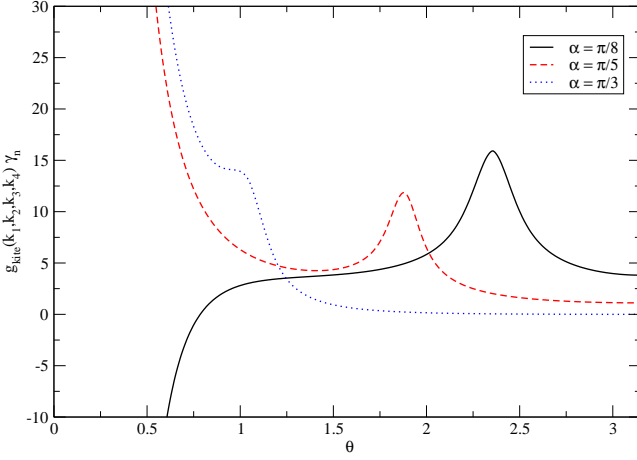


FIG. 2: Trispectrum geometrical factor for the kite quadrilaterals as a function of  $\theta$ , plotted for various values of  $\alpha$ . The trispectrum is enhanced in the squeezed limit  $\theta \rightarrow 0$ . The bump for  $\theta_p = \pi - 2\alpha$  corresponds to the parallelogram limit for which the unconnected part is no longer vanishing.

leading terms of the previous expression are

$$g_{\theta \ll 1} \sim \frac{8 \cos^2(\alpha)}{k^\rho \theta^{\rho-3}} (1 - 2 \cos 2\alpha) \times \left\{ 2(1 + \chi) \tan^2(\alpha) - 1 + 4^\chi (1 - \tan^2 \alpha) \right\}^{-1/(2\chi+2)}. \quad (58)$$

The sign of the kite trispectrum is the same as  $1 - 2 \cos(2\alpha) \cos(\theta)$  and, at small  $\theta$ , is negative for  $\alpha < \pi/6$  and positive otherwise. As for the bispectrum, we recover that squeezed configurations are the most sensitive to a string signal, certainly due to the elongated temperature discontinuities induced by the GKS effect. In Fig. 2, we have represented the full geometrical dependency coming from Eq. (54) as a function of  $\theta$  and for various values of  $\alpha$ . For convenience, we have chosen  $\chi = 0.29$ ,  $c_2 = 1$ ,  $k = 1$  and  $L = 20$ . The incomplete gamma function contributes for configurations close to the parallelogram ones which appear as a bump in Fig. 2 for  $\theta_p = \pi - 2\alpha$ . For the kites, the argument of the gamma function simplifies to

$$c_2 Y^2 \Lambda^{2\chi+2} = k^2 \frac{c_1 \hat{\xi}^2}{2(2\chi+1)(2\chi+2)} \left( \frac{2L}{\hat{\xi}} \right)^{2\chi+2} y^2(\theta, \alpha) \times \frac{[1 - 2 \cos(2\alpha) \cos(\theta)]^{-2(\chi+1)}}{\{2 \sin(\theta) + [\cos(\theta) - 1] \tan(\alpha)\}^{2(\chi+1)}}. \quad (59)$$

As can be seen on this plot, we recover the change of sign when  $\alpha$  crosses the value  $\pi/6$ . The bump at  $\theta_p = \pi - 2\alpha$  corresponds to the parallelogram limit of the kite configuration for which  $y^2(\theta, \alpha) \rightarrow 0$ .

## B. Trapezium

Let us next consider a quadrilateral given by the right side of Fig.1 having two opposite sides parallel. Without loss of generality, one can assume that the upper side is of smaller length than the bottom. Denoting their ratio by  $\sin^2(\beta)$ , after some algebra, the factor  $Y^2$  is still given by Eq. (55) with

$$y^2(\theta, \alpha) = [\sin^2(\theta)]^{\chi+1} \left[ \frac{\sin^2(\alpha + \theta)}{\sin^2(\alpha)} \right]^{\chi+2} \times \frac{1 - [\cos^2(\beta)]^{2\chi+1} - [\sin^2(\beta)]^{2\chi+1}}{\tan^2(\beta) [\sin^2(\beta)]^{2\chi+2}}. \quad (60)$$

Similarly, the geometrical factor reads

$$g(\mathbf{k}_1, \mathbf{k}_2, \mathbf{k}_3, \mathbf{k}_4) = \frac{\sin(\alpha) \sin(\theta) - 3 \cos(\alpha) \cos(\theta)}{k^\rho} \times \frac{\sin(\alpha)}{\sin^2(\theta)} \left[ \frac{\sin^2(\alpha)}{\sin^2(\alpha + \theta)} \right]^{(\rho-3)/2} \frac{\sin^4(\beta) [\tan^2(\beta)]^{(\rho-4)/2}}{\left\{ 1 - [\cos^2(\beta)]^{2\chi+1} - [\sin^2(\beta)]^{2\chi+1} \right\}^{-1/(2\chi+2)}}. \quad (61)$$

As expected, the trapezium trispectrum decays with the power-law exponent  $k^{-\rho}$ . The overall amplitude is again amplified for elongated configurations and diverges for  $\theta \rightarrow 0$ . For convex quadrilaterals, assuming  $0 < \theta < \pi - \alpha$ , the sign of the trispectrum is given by the first term of Eq. (61). As a result, it is negative for  $\theta < \theta_s$  and positive otherwise, where  $\theta_s$  is given by

$$\theta_s = \arccos \left[ \frac{\sin(\alpha)}{\sqrt{9 \cos^2(\alpha) + \sin^2(\alpha)}} \right]. \quad (62)$$

For an isosceles trapezium with  $\alpha = \theta$ , the change of sign occurs at  $\theta_s = \pi/3$ . Finally, in Fig. 3, we have plotted the full geometrical dependence as a function of  $\theta$ , for various values of  $\alpha$ . For the trapeziums, the argument of the gamma function is

$$c_2 Y^2 \Lambda^{2\chi+2} = k^2 \frac{c_1 \hat{\xi}^2}{2(2\chi+1)(2\chi+2)} \left( \frac{2L}{\hat{\xi}} \right)^{2\chi+2} y^2(\theta, \alpha) \times [\sin(\alpha) \sin(\theta) - 3 \cos(\alpha) \cos(\theta)]^{-2(\chi+1)} \times \left\{ \frac{\sin(\theta) \sin(\theta + \alpha) [3 + \cos^2(\beta)]}{\sin(\alpha) \sin^2(\beta)} \right\}^{-2(\chi+1)}. \quad (63)$$

The divergence for the parallelograms visible at  $\theta = \pi - \alpha$  comes again from the squeezed shape. Imposing a fixed value of  $\sin^2(\beta)$  implies that such parallelograms are infinitely elongated. The configuration with  $\theta > \pi - \alpha$  are self-intersecting trapeziums having a butterfly shape. Their squeezed limit occurs for  $\theta \rightarrow \pi$  for which the trispectrum is again strongly enhanced.

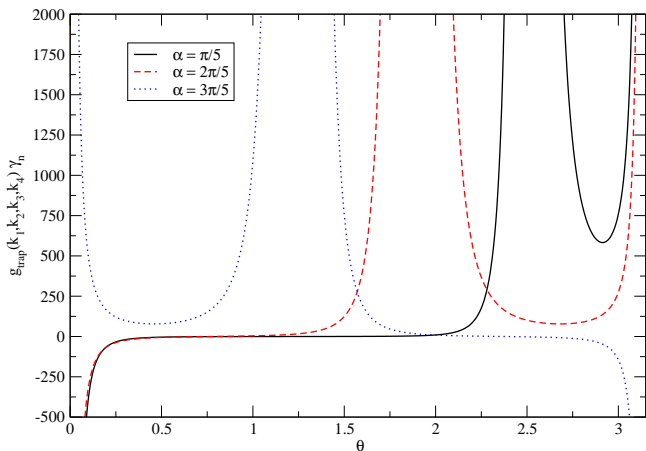


FIG. 3: Trispectrum geometrical factor for the trapezium quadrilaterals as a function of  $\theta$ , plotted for various values of  $\alpha$ . For convenience, the ratio of the two parallel sides has been fixed to  $3/4$  and  $\chi = 0.29$ . The divergence in the squeezed limit occurs at  $\theta \rightarrow 0$  but also at  $\theta_p = \pi - \alpha$  for infinitely elongated parallelograms. For  $\theta > \theta_p$ , the trapeziums are no longer convex and represent “butterfly” configurations which are squeezed for  $\theta \rightarrow \pi$ .

## V. CONCLUSION

In this paper, we have analytically derived the CMB temperature trispectrum induced by cosmic strings using the string correlation functions in the Gaussian approximation. The trispectrum generically decays with a non-integer power-law behaviour at small angular scales which depends on the string microstructure through the behaviour of the tangent vector correlator on small distances. Its eventual detection and measurement may therefore help to distinguish between different string models. We have also found that the trispectrum diverges, in the framework of our approximations, on all squeezed configurations whose measurements remain however limited by the finite experimental resolution. In

fact, such a non-integer power-law is linked to the existence of a “flat direction” at leading order and the four-point function ends up being sensitive to the next-to-leading order string tangent vector correlator. This situation is also present in the  $n$ -point function and we do expect all of the higher  $n$ -point function to exhibit non-integer power-law behaviours. Since this situation was not encountered for the two- and three-point functions, the next step will be to compare our results here with the trispectrum computed from CMB maps obtained by string network simulations.

Finally, let us notice that we have not attempted to make any comparison with a CMB trispectrum produced by primordial non-Gaussianities of inflationary origin. The situation is nearly the same as it is for the string bispectrum [22]. The so-called  $\tau_{\text{NL}}$  and  $g_{\text{NL}}$  parameters quantify the amplitude of the primordial four-point function of the curvature perturbation on super-Hubble scales. As a result, the induced trispectrum of the CMB temperature fluctuations strongly depends on the CMB transfer functions and exhibits damped oscillations with respect to the multipole moments. Here, we have directly derived the CMB temperature trispectrum produced by the strings and it would therefore make no sense to find an associated  $\tau_{\text{NL}}$  and  $g_{\text{NL}}$ . An alternative approach might be to estimate what values  $\tau_{\text{NL}}$  and  $g_{\text{NL}}$  would assume in a primordial-type oriented data analysis if the non-Gaussianities were actually due to strings. This could be done with a Fisher matrix analysis for a given experiment but we leave this question for a forthcoming work.

## Acknowledgments

This work is partially supported by the Belgian Federal Office for Scientific, Technical, and Cultural Affairs through the Inter-University Attraction Pole Grant No. P6/11.

- 
- [1] T. W. B. Kibble, *J. Phys.* **A9**, 1387 (1976).
  - [2] A. Dabholkar, G. W. Gibbons, J. A. Harvey, and F. Ruiz Ruiz, *Nucl. Phys.* **B340**, 33 (1990).
  - [3] M. B. Hindmarsh and T. W. B. Kibble, *Rept. Prog. Phys.* **58**, 477 (1995), hep-ph/9411342.
  - [4] A. Vilenkin and E. P. S. Shellard, *Cosmic Strings and Other Topological Defects* (Cambridge University Press, Cambridge, 1994).
  - [5] L. Kofman, A. D. Linde, and A. A. Starobinsky, *Phys. Rev. Lett.* **73**, 3195 (1994), hep-th/9405187.
  - [6] J. Yokoyama, *Phys. Rev. Lett.* **63**, 712 (1989).
  - [7] M. Sakellariadou, *Lect. Notes Phys.* **718**, 247 (2007), hep-th/0602276.
  - [8] E. J. Copeland, R. C. Myers, and J. Polchinski, *JHEP* **06**, 013 (2004), hep-th/0312067.
  - [9] S. Sarangi and S. H. H. Tye, *Phys. Lett.* **B536**, 185 (2002), hep-th/0204074.
  - [10] G. Dvali and A. Vilenkin, *JCAP* **0403**, 010 (2004), hep-th/0312007.
  - [11] J. R. Gott III, *Astrophys. J.* **288**, 422 (1985).
  - [12] N. Kaiser and A. Stebbins, *Nature* **310**, 391 (1984).
  - [13] E. Jeong and G. F. Smoot, *Astrophys. J.* **624**, 21 (2005), astro-ph/0406432.
  - [14] E. Jeong and G. F. Smoot, *Astrophys. J. Lett.* **661**, L1 (2007), arXiv:astro-ph/0612706.
  - [15] J. L. Christiansen et al., *Phys. Rev.* **D77**, 123509 (2008), 0803.0027.
  - [16] F. R. Bouchet, P. Peter, A. Riazuelo, and M. Sakellariadou, *Phys. Rev.* **D65**, 021301(R) (2001), astro-ph/0005022.

- [17] R. A. Battye, B. Garbrecht, and A. Moss, JCAP **0609**, 007 (2006), astro-ph/0607339.
- [18] N. Bevis, M. Hindmarsh, M. Kunz, and J. Urrestilla (2007), astro-ph/0702223.
- [19] A. A. Fraisse, C. Ringeval, D. N. Spergel, and F. R. Bouchet, Phys. Rev. **D78**, 043535 (2008), 0708.1162.
- [20] U. Seljak and A. Slosar, Phys. Rev. D **74**, 063523 (2006), arXiv:astro-ph/0604143.
- [21] K. Takahashi et al., JCAP **0910**, 003 (2009), 0811.4698.
- [22] M. Hindmarsh, C. Ringeval, and T. Suyama, Phys. Rev. **D80**, 083501 (2009), 0908.0432.
- [23] W. Hu, Phys. Rev. **D64**, 083005 (2001), astro-ph/0105117.
- [24] M. Hindmarsh, Astrophys. J. **431**, 534 (1994), astro-ph/9307040.
- [25] J. Polchinski and J. V. Rocha, Phys. Rev. **D74**, 083504 (2006), hep-ph/0606205.
- [26] E. J. Copeland and T. W. B. Kibble, Phys. Rev. **D80**, 123523 (2009), 0909.1960.
- [27] C. Ringeval, M. Sakellariadou, and F. Bouchet, JCAP **0702**, 023 (2007), astro-ph/0511646.
- [28] J. V. Rocha, Phys. Rev. Lett. **100**, 071601 (2008), 0709.3284.
- [29] D. Austin, E. J. Copeland, and T. W. B. Kibble, Phys. Rev. **D48**, 5594 (1993), hep-ph/9307325.
- [30] F. Dubath, J. Polchinski, and J. V. Rocha, Phys. Rev. **D77**, 123528 (2008), 0711.0994.
- [31] M. Hindmarsh, S. Stuckey, and N. Bevis, Phys. Rev. **D79**, 123504 (2009), 0812.1929.
- [32] D. P. Bennett and F. R. Bouchet, Phys. Rev. D **41**, 2408 (1990).